Oncology Research, Vol. 27, pp. 147–155
Printed in the USA.

0965-0407/19 $90.00 + .00
DOI: https://doi.org/10.3727/096504017X15021536183517
E-ISSN 1555-3906
www.cognizantcommunication.com

miR-26b Mimic Inhibits Glioma Proliferation In Vitro and In Vivo Suppressing COX-2 Expression

Zheng-Gang Chen,* Chuan-Yi Zheng,* Wang-Qing Cai,† Da-Wei Li,* Fu-Yue Ye,* Jian Zhou,* Ran Wu,* and Kun Yang*

*Department of Neurosurgery, The First Affiliated Hospital of Hainan Medical College, Haikou, Hainan, P.R. China
†Department of Neurosurgery, The Sun Yat-Sen Memorial Hospital of Sun Yat-Sen University, Guangzhou, Guangdong, P.R. China

Glioma is the most common malignant tumor of the nervous system. Studies have shown the microRNA-26b (miR-26b)/cyclooxygenase-2 (COX-2) axis in the development and progression in many tumor cells. Our study aims to investigate the effect and mechanism of the miR-26b/COX-2 axis in glioma. Decreased expression of miR-26b with increased levels of COX-2 was found in glioma tissues compared with matched normal tissues. A strong negative correlation was observed between the level of miR-26b and COX-2 in 30 glioma tissues. The miR-26b was then overexpressed by transfecting a miR-26b mimic into U-373 cells. The invasive cell number and wound closing rate were reduced in U-373 cells transfected with miR-26b mimic. In addition, COX-2 siRNA enhanced the effect of miR-26b mimic in suppressing the expression of p-ERK1 and p-JNK. Finally, the in vivo experiment revealed that miR-26b mimic transfection strongly reduced the tumor growth, tumor volume, and expression of matrix metalloproteinase-2 (MMP-2) and MMP-9. Taken together, our research indicated a miR-26b/COX-2/ERK/JNK axis in regulating the motility of glioma in vitro and in vivo, providing a new sight for the treatment of glioma.

Key words: MicroRNA 26b (miR-26b); Glioma; Cyclooxygenase 2 (COX-2); Invasion; Migration; Extracellular signal-regulated kinase (ERK)

INTRODUCTION

Glioma is the most common malignant tumor of the nervous system. Its incidence is about 40%–60% among the intracranial tumors[1]. The main features of gliomas are the difficulty to control proliferation and extensive infiltration of surrounding tissues[2]. Until now, no clear boundary between glioma tissue and normal brain tissue has been indicated. In recent years, there has been great progress in the comprehensive treatment of chemotherapy and radiotherapy. However, the overall survival time of glioma patients has not been significantly improved[3,4]. Therefore, the study of the mechanism of glioma proliferation and the invasion or screening of molecular targets is the focus of the current study of glioma.

MicroRNAs (miRNAs) may play an important role in promoting cancer or inhibiting cancer in the process of tumorigenesis[5]. miRNAs are widely involved in the regulation of gene expression, cell cycle, and biological development[6]. Many studies have shown that miRNAs are closely related to many tumors and are closely related to tumor invasion and metastasis, such as breast cancer[7], liver cancer[8], colon cancer[9], and lung cancer[10]. miR-26b is located in the human chromosome 2q35. It is located in the fourth intron of the C-terminal domain small phosphatase 1 (CTDSP1) gene[11]. Many studies have shown that miR-26b plays an inhibiting role in the development and progression of many cancers[12,13]. However, the expression of miR-26b in glioma and its role in the proliferation and invasion of glioma cells are rarely reported.

Cyclooxygenase (COX) is the key rate-limiting enzyme in the conversion of arachidonic acid to prostaglandins[14]. COX-2 is located on human chromosome 1 q25.2-q25.3[15]. COX has two kinds of isozymes, namely, COX-1 and COX-2. Under normal physiological conditions, COX-2 is almost impossible to detect. However, when the cells are stimulated by inflammatory signals or some cytokines, the expression of COX-2 will be increased significantly[16]. Many studies have shown that

Address correspondence to Kun Yang, Department of Neurosurgery, The First Affiliated Hospital of Hainan Medical College, No. 23 Longhua Road, Longhua District, Haikou, Hainan 570102, P.R. China. E-mail: kunyangsyu@sina.com

COX-2 expression was increased in many tumors. The high expression of COX-2 is closely related to the high invasiveness of lung cancer[17], colon cancer[18], liver cancer[19], and other tumor cells[20]. The study of Fujita et al. has shown that the expression of COX-2 in glioma was significantly increased and was closely related to the invasion ability of glioma cells[21].

Therefore, this study intends to clarify the interaction between miR-26b and COX-2. The role and mechanism of miR-26b in the invasion and migration of glioma cells were further clarified.

MATERIALS AND METHODS

Cell Lines and Main Reagents

Human glioma cell lines U-87, C6, U-373, and M059J and human astrocytes were purchased from the American Type Culture Collection (Manassas, VA, USA). Cell culture conditions were Roswell Park Memorial Institute (RPMI) or Dulbecco's modified Eagle's medium (DMEM) containing 10% fetal bovine serum (FBS), at 37°C, 5% CO_2. FBS, RPMI, and DMEM were purchased from Gibco (Rockville, MD, USA). COX-2, extracellular signal-regulated kinase1 (ERK1), phosphorylated (p)-ERK1, c-Jun N-terminal kinase (JNK), and p-JNK were purchased from Abcam (Cambridge, UK). The Transwell chamber was purchased from Corning (Corning, NY, USA). Matrigel was purchased from Bio-Rad (Hercules, CA, USA). Nude mice [6 weeks old, specific pathogen free (SPF)] were provided by the experimental animal center of Sichuan University. TRIzol was purchased from Invitrogen (Carlsbad, CA, USA). Reverse transcription kits (FSQ-101) were purchased from TOYOBO Company (Kyoto, Japan). Lipofectamine 2000 and miR-26b mimic were purchased from Ji Kai Gene Company (Shanghai, P.R. China). Luciferase activity assay kit and luciferase reporter vectors were purchased from Promega (Madison, WI, USA).

Quantitative RT-PCR (qRT-PCR)

Total RNA from glioma tissues and cell lines was harvested using the TRIzol reagent (Invitrogen) following the manufacturer's instructions. Total RNA was eluted with RNase-free water and stored at −80°C. RNAs were reverse transcribed into cDNAs using the RT-PCR kit purchased from TaKaRa (Dalian, China) according to the manufacturer's protocol. SYBR Premix Ex Taq (TaKaRa) was used to detect COX-2 and miR-26b according to the manufacturer's protocol. The RT-PCR primers for COX-2 and miR-26b were purchased from GeneCopoeia (San Diego, CA, USA). The specific primers were as follows: COX-2, 5 -CTTGGGTGTCAAAGGTAA-3 (forward) and 5 -AGGGACTTGAGGAGGGTA-3 (reverse); miR-26b, 5 -CGCCCTGTTCTCCATTACTT-3 (forward) and 5 -C CAGTGCAGGGTCCGAGGT-3 (reverse). GAPDH and U6 small nuclear RNA (snRNA) were used as the internal control of the messenger RNA (mRNA) or miRNA, respectively. Fold change of COX-2 or miR-26b was calculated by the equation 2^{-} Ct.

Cell Transfection

Mimics/inhibitors specific for miR-26b, mimic/scramble fragments, and siRNA COX-2 were designed and purchased from Invitrogen. U-373 cells were seeded in 24-well plates at 1 10^5 cells per well. Transfections were performed using Lipofectamine® 2000 (Invitrogen; Thermo Fisher Scientific, Inc.) for 24 h. After transfection, the cells were allowed to recover by incubating them for 4 h at 37°C. The experiment was replicated three times for data calculations according to the manufacturer's protocol. The expression of miR-26b was detected by qPCR after transfection.

Luciferase Activity Assay

U-373 cells were cotransfected with luciferase reporter vector and miR-26b mimics. The pGL-TK was taken as the standard control. After transfection for 36 h, the cells were harvested. The luciferase activity of U-373 cells was measured by Promega's luciferase assay kit. Relative luciferase activity = firefly luciferase activity/luciferase activity value of sea kidney. The experiment was repeated three times.

Western Blotting

Total protein was extracted from U-373 cells, and 20 μg of isolated protein was separated by SDS-PAGE) and transferred onto a polyvinylidene fluoride (PVDF) membrane (Millipore, Billerica, MA, USA). The membranes were blocked in phosphate-buffered saline (PBS) with 0.1% Tween 20 containing 5% nonfat milk for 2 h at room temperature and then were incubated with the primary antibodies: anti-COX-2, anti-ERK1, anti-p-ERK1, anti-JNK, anti-p-JNK, and anti-GAPDH, and the corresponding horseradish peroxidase (HRP)-conjugated secondary antibodies, followed by detection and visualization using a ChemiDoc XRS imaging system and analysis software (Bio-Rad, San Francisco, CA, USA). U6 and GAPDH (Abcam) were used as endogenous references.

Northern blotting

The expression levels of miR-26b in U-373 cells transfected with mimic control or miR-26b mimic were further determined by Northern blot assay. Northern blot analysis was performed as previously described[22]. U6 (Abcam) was used as endogenous reference.

Fluorescence Microscopy

U-373 cells were transfected with green fluorescent protein (GFP) plasmid by Lipofectamine 3000™

(Invitrogen). After U-373 cells were treated with or without miR-26b and mimic, the number of puncta formation of GFP was determined under fluorescence microscopy.

Transwell Invasion Assay

Two Transwell invasion chambers with Matrigel (1 mg/ml; Becton-Dickinson, Franklin Lakes, NY, USA) were used in invasion assays of U-373 cells in vitro. First, 200 µl of serum-free medium containing 1 10^5 cells/well was added into the upper chamber, and the lower chamber contained 0.6 ml of medium containing 20% FBS. After incubation at 37°C for 24 h, noninvading cells on the upper membranes were removed with a cotton swab. The migrated or invaded cells were fixed in 95% ethanol and stained with hematoxylin. The cell numbers were counted by the ImageJ software (NIH, Bethesda, MD, USA) and photographed under an inverted microscope in 10 random fields from each well. Each experiment was independently repeated in triplicate.

Wound Healing Assay

Wound healing assay was performed to evaluate the migration rate of U-373 cells transfected with or without miR-26b mimic. To accomplish this, 1.5 10^6 cells/well were seeded in six-well plates and cultured overnight until the cells reached 90% confluence. A straight scratch was created by a sterile pipette tip. The destroyed cells were gently rinsed off with PBS three times and cultured in medium for another 24 h. Cell migration was observed and imaged at 0 and 24 h with a digital camera (Leica DFC300FX; Wetzlar, Germany).

Glioma Xenografts

SPF athymic nude mice (male, 6 to 8 weeks of age) were purchased from the experimental animal center of Sichuan University. Mice were housed and manipulated according to the protocols approved by the Experimental Animal Center of the Hainan Medical College. For researching tumorigenicity of miR-26b mimic in vivo, a xenograft mouse model was created by subcutaneous injection of 1 10^7 U-373 cells transfected with or without miR-26b mimic to SPF nude mice. After the development of a palpable tumor, the tumor volume was monitored every 5 days and assessed by measuring the two perpendicular dimensions using a caliper and the formula (a b^2)/2, where a is the larger and b is the smaller dimension of the tumor. At 30 days after inoculation, the mice were killed, and tumor weights were assessed. Tumors from each mouse were randomly selected for immunohistochemical (IHC) analysis. All the animal experiments were performed according to relevant national and international guidelines and were approved by the Animal Experimental Ethical Committee.

Immunohistochemistry

Formalin-fixed paraffin-embedded U-373 tumors were cut with a microtome into 5-µm-thick paraffin sections. Antigen retrieval was carried out in heated 10 mM citrate buffer of pH 6.0 for 10 min at 96°–98°C. Slides were incubated with primary antibodies against matrix metalloproteinase-2 (MMP-2) and MMP-9 (Boster Bioengineering, Wuhan, P.R. China). Corresponding mouse HRP-conjugated secondary antibody was added for 1 h at room temperature. Cells were counterstained with 10 mg/ml DAPI. Sections were subsequently incubated with the Cell and Tissue Staining Kit HRP-DAB system (R&D Systems, Minneapolis, MN, USA) according to the manufacturer's instructions.

Statistical Analysis

The quantitative data were expressed as mean ± SD. Statistical analysis was carried out using one-way analysis of variance (ANOVA) followed by Bonferroni test. Differences with a value of $p < 0.05$ were regarded as statistically significant.

RESULTS

Inversed Expression Level of miR-26b and COX-2 Was Observed in Glioma Tissues and Cell Lines

The expression levels of miR-26b and COX-2 were detected in glioma tissues and matched adjacent normal tissues by qRT-PCR. The results indicated that the level of miR-26b was significantly lower in glioma tissues compared with normal tissues ($p < 0.01$) (Fig. 1A). Conversely, the mRNA expression level of COX-2 was increased in glioma tissues compared with normal tissues ($p < 0.01$) (Fig. 1B), and there was a strong negative correlation between the expression level of miR-26b and the mRNA expression level of COX-2 in glioma tissues ($p < 0.0001$) (Fig. 1C). In addition, the expression level of miR-26b and COX-2 was also detected in four glioma cell lines (U-87, C6, U-373, and M059J) and in human astrocytes by qRT-PCR. The results indicated that the level of miR-26b was significantly lower in glioma cells compared with astrocytes ($p < 0.01$) (Fig. 1D). The mRNA and protein expression levels of COX-2 were examined by qRT-PCR and Western blot analysis, respectively. The results showed that both the mRNA and protein levels of COX-2 were significantly elevated in glioma cell lines compared with human astrocytes ($p < 0.01$) (Fig. 1E–G). These results indicate that the level of miR-26b was decreased with elevated level of COX-2 in glioma.

miR-26b Mimic Inhibits the Expression of COX-2

Considering the low expression of miR-26b in glioma cells, a miR-26b mimic was transfected into U-373 cells to enhance the expression of miR-26b. As shown in

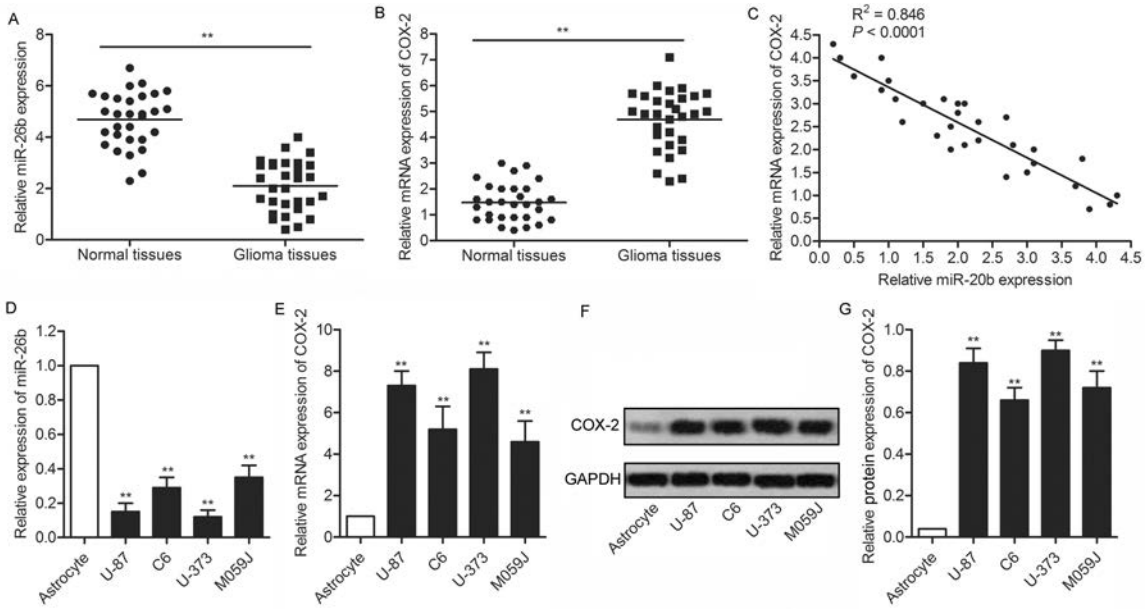

Figure 1. Inversed expression level of microRNA-26b (miR-26b) and cyclooxygenase-2 (COX-2) was observed in glioma tissues and cell lines. (A) The expression levels of miR-26b in glioma tissues and matched adjacent normal tissues by quantitative (q)RT-PCR. (B) The messenger RNA (mRNA) expression of COX-2 in glioma tissues and matched adjacent normal tissues was assessed by qRT-PCR assays. (C) The correlation between miR-26b expression levels and COX-2 mRNA expression levels in glioma tissues. (D) The expression levels of miR-26b in four glioma cell lines (U-87, C6, U-373, and M059J) and human astrocytes were measured by qRT-PCR. (E) The mRNA expression of COX-2 in glioma cell lines and astrocytes was assessed by qRT-PCR. (F) Western blotting assay was used to detect the expression profile of COX-2 in glioma cell lines and astrocytes. (G) Relative protein expression was quantified using Image-Pro Plus 6.0 software and normalized to GAPDH. Data are represented as the mean ± SD of three experiments. $^{**}p < 0.05$ versus controls group.

Figure 2A, the expression of miR-26b was strongly promoted in U-373 cells transfected with miR-26b mimic compared with the control group ($p < 0.001$) (Fig. 2A). The results of cell fluorescence indicated that miR-26b mimic was well integrated in glioma cells with high transfection efficiency (Fig. 2B). The mRNA expression level of COX-2 was decreased significantly in U-373 cells transfected with miR-26b mimic compared with control group ($p < 0.001$) (Fig. 2C). The elevated level of miR-26b and the decreased protein expression level of COX-2 were further confirmed by Northern blot and Western blot (Fig. 2D and E). These results suggest that miR-26b mimic transfection inhibits the expression of COX-2.

COX-2 Is a Direct Target of miR-26b

As predicted by TargetScan, COX-2 is a target of miR-26b (Fig. 3A). To determine the targeting relationship between miR-26b and COX-2, miR-26b mimic/COX-2 wild type (Wt)/COX-2 mutant (Mut) was transfected into U-373 cells. According to the luciferase reporter assays, miR-26b mimic significantly inhibited the luciferase activity of COX-2 Wt, whereas miR-26b mimic had no significant inhibitory effect on COX-2 Mut luciferase ($p < 0.001$) (Fig. 3B). These results indicate that COX-2 is a direct target of miR-26b.

miR-26b Mimic Suppresses the Invasion and Migration of U-373 Cells

We next investigated the effect of miR-26b in the motility of glioma. Treatment of the miR-26b mimic significantly decreased the invasive cells of U-373 cells compared with the control group ($p < 0.01$) (Fig. 4A and B). Overexpression of miR-26b decreased the wound closing rate of U-373 cells compared with the control group ($p < 0.01$) (Fig. 4C and D). These results indicate that miR-26b overexpression suppresses the motility of glioma.

miR-26b Mimic Inactivates the ERK/JNK Pathway

As shown in Figure 5, the expression levels of COX-2 were significantly decreased in U-373 cells transfected with COX-2 siRNA compared with the control group ($p < 0.05$). The levels of p-ERK1 and p-JNK were significantly decreased in U-373 cells transfected with miR-26b mimic or COX-2 siRNA compared with control group ($p < 0.05$). The expression level of ERK1 and JNK exhibited no obvious change. COX-2 siRNA enhanced the suppressing effect of miR-26b mimic transfection on the expression of p-ERK1 and p-JNK ($p < 0.05$). These results suggest that miR-26b mimic and COX-2 siRNA can inactivate the ERK/JNK pathway.

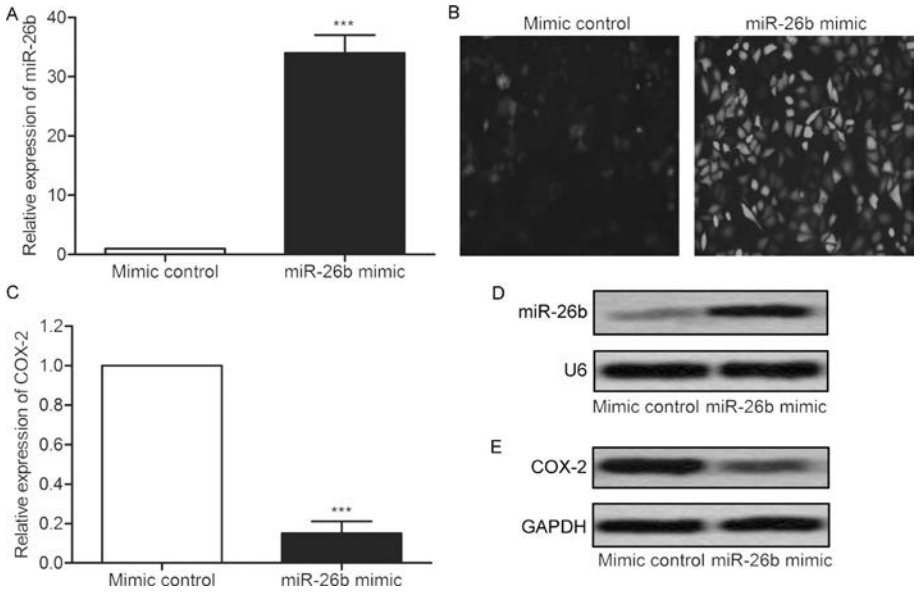

Figure 2. miR-26b mimic inhibits the expression of COX-2. U-373 cells were transfected with miR-26b mimic or mimic control, respectively. (A) The relative miR-26b levels in U-373 cells were measured by qRT-PCR. (B) The transfection efficiency was detected by green fluorescent protein (GFP) fluorescence (original magnification: 400). (C) The relative mRNA expression level of COX-2 in U-373 cells was measured by qRT-PCR. (D) The level of miR-26b was detected by Northern blot. (E) The level of COX-2 was measured by Western blot. All experiments were repeated three times with three replicates. ***$p < 0.001$ versus mimic control group.

miR-26b Mimic Impairs Tumor Growth In Vivo

Transfection of miR-26b mimic effectively suppressed tumor formation and tumor volume compared with the control group (Fig. 6A and B). The expression of miR-26b and COX-2 was detected through Northern blotting and Western blot, respectively. The level of miR-26b was increased with downregulation of COX-2 in the glioma model mice transfected with miR-26b mimic compared with control group (Fig. 6C). The expression of p-ERK1 and p-JNK was also inhibited by miR-26b mimic transfection (Fig. 6D). The production of MMP-2 and MMP-9 was significantly reduced in mice with miR-26b mimic transfection ($p < 0.001$) (Fig. 6E). These results indicate that miR-26b mimic transfection inhibits the tumor growth of glioma in vivo.

DISCUSSION

Research shows that miR-26b plays a role in tumor suppression in a variety of tumors and plays an important role in the processes of tumor cell proliferation, invasion,

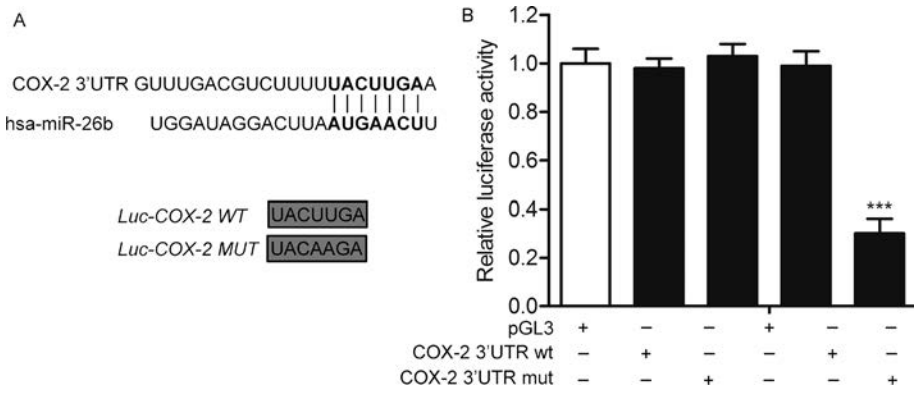

Figure 3. COX-2 is a direct target of miR-26b. (A) The target gene of miR-26b was predicted by the TargetScan database. The wild-type (Wt) and the mutant (Mut) COX-2 3 -UTR contained the target sequence of miR-26b. (B) Luciferase assay was performed in U-373 cell lines treated with miR-26b mimic or mimic control. Luciferase activity was represented as firefly luciferase normalized to *Renilla* luciferase. Data are represented as the mean ± SD of three experiments. ***$p < 0.001$ versus mimic control group.

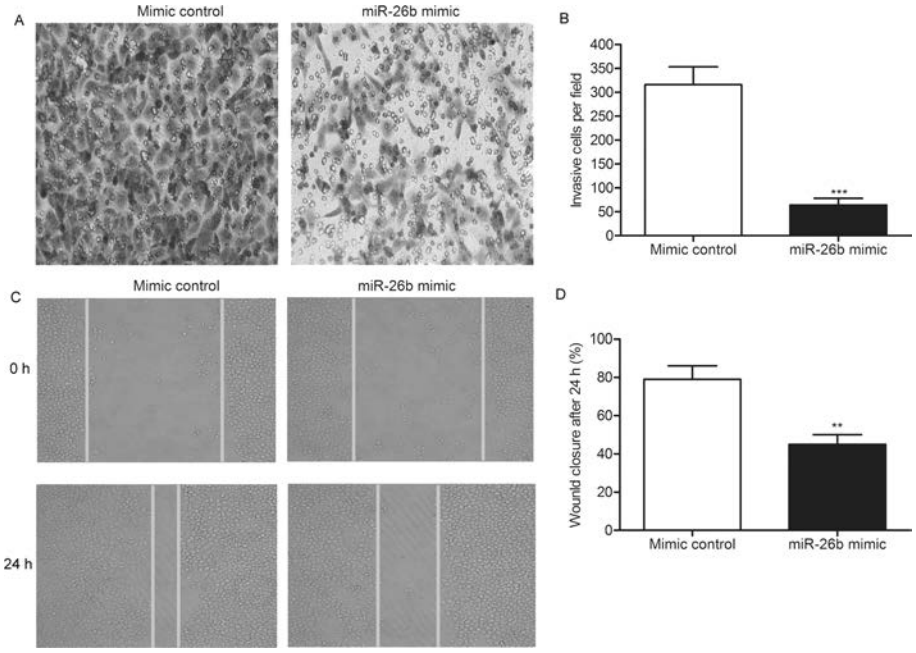

Figure 4. miR-26b mimic suppresses the invasion and migration of U-373 cells. (A) The invasive cells were detected by Transwell invasion assays in U-373 cells transfected with miR-26b mimic or mimic control. (B) Histogram represents the statistical analysis of Transwell invasion assays. (C) The migration rate of U-373 cells was measured by wound healing assays. (D) Histogram represents the statistical analysis of wound healing assays. The bars show means ± SD of three independent experiments. $^{**}p < 0.01$, $^{***}p < 0.001$ indicate significant difference.

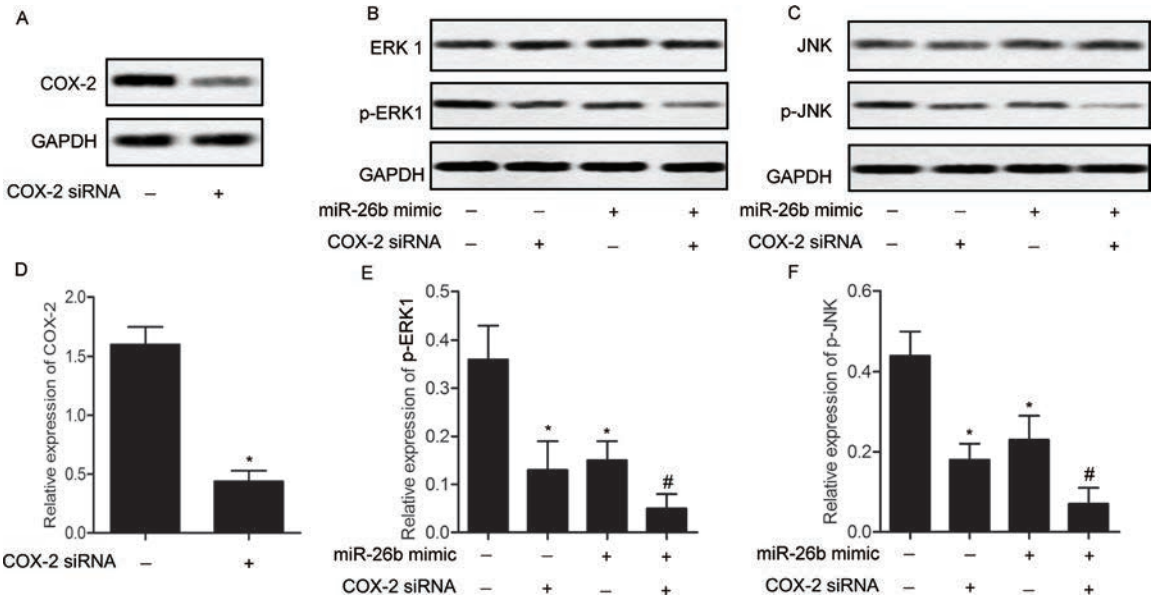

Figure 5. miR-26b mimic inactivates the extracellular signal-regulated kinase (ERK)/c-Jun N-terminal kinase (JNK) pathway. U-373 cells were transfected with COX-2 siRNA. The protein expression of COX-2 was detected by Western blotting (A). U-373 cells were then transfected with miR-26b mimic with/or without COX-2 siRNA. The protein expression levels of ERK1 (B), JNK (C), and their phosphorylated forms were detected in U-373 cells by Western blotting. Relative protein expression levels of COX-2 (D), p-ERK1 (E), and p-JNK (F) in U-373 cells were quantified using Image-Pro Plus 6.0 software and normalized to GAPDH. Data are represented as the mean ± SD of three experiments. $^{*}p < 0.05$ versus control group, $\#p < 0.05$ versus miR-26b mimic group.

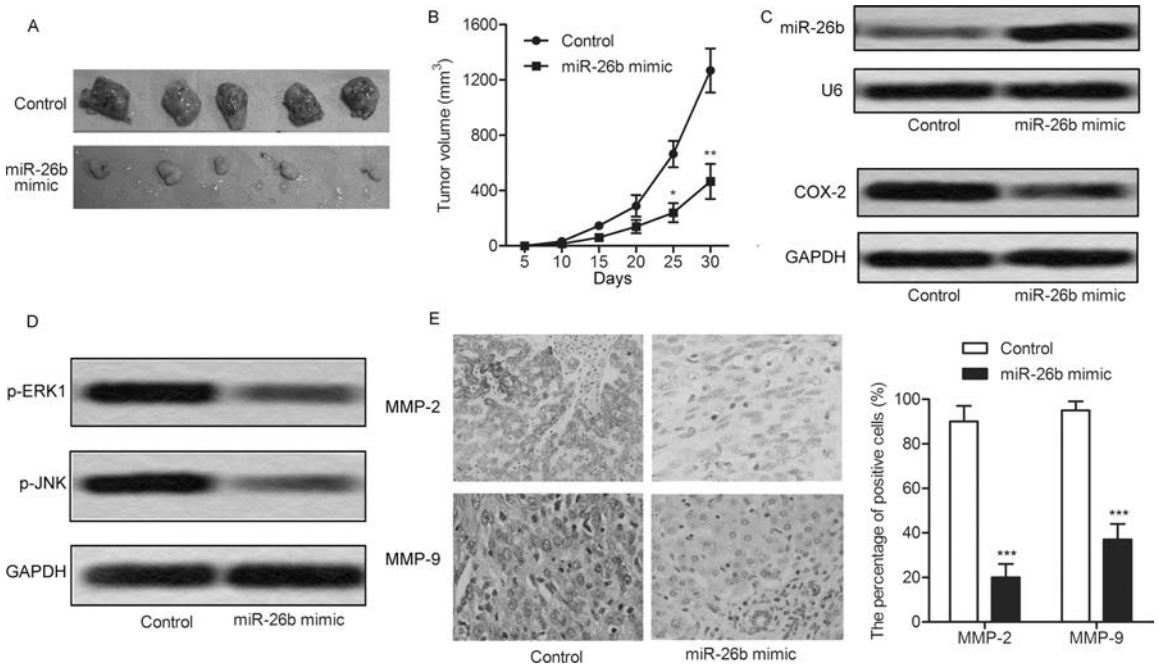

Figure 6. miR-26b mimic restrains tumor growth in vivo. The glioma xenograft mouse model was created by subcutaneous injection of U-373 cells pretreated with or without miR-26b mimic to specific pathogen-free (SPF) nude mice. (A) Representative tumors from the two groups of mice are shown ($n=5$). (B) Tumor growth trend in lncRNA COX-2 mice and control group mice is shown. The expression of miR-26b, COX-2 (C), p-ERK1, and p-JNK (D) was detected in the glioma model mice by Northern blot or Western blot. (E) The production of matrix metalloproteinase-2 (MMP-2) and MMP-9 was detected by immunohistochemistry. *$p<0.05$, **$p<0.01$, ***$p<0.001$ versus control group.

and metastasis[23]. Verghese et al. found that the expression of miR-26b was decreased in breast cancer, and miR-26b inhibited the invasion and migration abilities of breast cancer cells[11]. Shen et al. indicated that the level of miR-26b was significantly decreased in hepatocellular carcinoma (HCC) tissues than the adjacent tissues[24]. The expression level of miR-26b was negatively correlated with the staging and grading of liver cancer and lymph node metastasis. In our study, the expression of miR-26b was significantly decreased in glioma tissues compared with matched adjacent normal tissues. The decreased level of miR-26b was also observed in glioma cell lines compared with human astrocytes. These results suggest that the low expression of miR-26b may be involved in the progression of glioma.

Many studies have shown that the expression of COX-2 is associated with tumor invasion and migration[18,21,25]. The possible mechanisms are the following. a) The high expression of COX-2 can promote the expression of E-cadherin cell adhesion molecules, and then promote tumor invasion and metastasis. Research has shown that COX-2 can activate the mitogen-activated protein kinase (MAPK)/ERK signaling pathway to promote the invasion and migration of tumor cells[26]. b) COX-2 can destroy the MMP inhibitor, resulting in increased expression of MMPs. The MMPs degrade the extracellular matrix, thus promoting the invasion and migration of tumor cells[27]. c) COX-2 can promote the angiogenesis of tumor cells and contribute to the invasion and migration of tumor cells[28]. In this study, the expression of COX-2 was significantly increased in glioma tissues compared with matched adjacent normal tissues. The elevated level of COX-2 was also observed in glioma cell lines compared with human astrocytes. In addition, miR-26b mimic transfection inhibited the expression of COX-2. The targeting relationship between miR-26b and COX-2 was confirmed by luciferase reporter assays.

MAPK is a serine/threonine protein kinase found in cells. It plays an important role in cell proliferation, apoptosis, and other physiological process[29]. The biological function of the MAPK signaling pathway is realized by the phosphorylation of MAPK kinase kinase (MAPKKK), MAPK kinase (MAPKK), and MAPK. Phosphorylation of some nuclear factors can be performed by MAPK to regulate the biological behavior and function of cells[30]. Studies have shown that the invasion and metastasis of breast cancer are related to the abnormal activation of the ERK/MAPK signaling pathway[31]. Protease-activated receptor-2 can induce the expression of vascular endothelial growth factor (VEGF) and COX-2 in gastric cancer

cells by activating ERK1/2 and p38 signaling pathways to promote the angiogenesis of gastric cancer cells[32]. In this study, the invasion and migration abilities of glioma cells were detected by Transwell and scratch assays after overexpression of miR-26b. The results showed that the invasion and migration abilities of glioma cells were significantly decreased after overexpression of miR-26b. The expression levels of p-ERK1 and p-JNK were significantly decreased in U-373 cells transfected with miR-26b mimic and COX-2 siRNA compared with the control group. These results indicate that the overexpression of miR-26b inhibits the motility of gliomas via targeting COX-2 and inactivating the ERK/JNK pathway.

Taken together, this study found that the level of miR-26b was decreased with the elevated level of COX-2 in glioma. miR-26b was then overexpressed by transfecting miR-26b mimic into glioma U-373 cells. COX-2 was demonstrated to be a direct target of miR-26b. The invasive cell number and the wound closing rate were reduced in U-373 cells transfected with miR-26b mimic compared with the control group. Moreover, the level of p-ERK1 and p-JNK was decreased significantly in U-373 cells transfected with miR-26b mimic and COX-2 siRNA. Finally, the in vivo experiment revealed that miR-26b mimic transfection strongly reduced the tumor growth, tumor volume, and MMP-2^+/MMP-9^+ cell numbers. Our research indicated a miR-26b/COX-2/ERK/JNK axis. This axis may be a marker to predict progression and prognosis, and for monitoring any therapeutic effects of glioma.

ACKNOWLEDGMENT: This work was funded by the Natural Science Foundation of Hainan Province, P.R. China (No. 20168298). The authors declare no conflicts of interest.

REFERENCES

1. Kurzwelly D, Herrlinger U, Simon M. Seizures in patients with low-grade gliomas—Incidence, pathogenesis, surgical management, and pharmacotherapy. Adv Tech Stand Neurosurg. 2010;35:81–111.
2. Vakilian A, Khorramdelazad H, Heidari P, Sheikh Rezaei Z, Hassanshahi G. CCL2/CCR2 signaling pathway in glioblastoma multiforme. Neurochem Int. 2017;103:1–7.
3. Kinnersley B, Mitchell JS, Gousias K, Schramm J, Idbaih A, Labussiere M, Marie Y, Rahimian A, Wichmann HE, Schreiber S, Hoang-Xuan K, Delattre JY, Nöthen MM, Mokhtari K, Lathrop M, Bondy M, Simon M, Sanson M, Houlston RS. Quantifying the heritability of glioma using genome-wide complex trait analysis. Sci Rep. 2015; 5:17267.
4. Sizoo EM, Pasman HR, Dirven L, Marosi C, Grisold W, Stockhammer G, Egeter J, Grant R, Chang S, Heimans JJ, Deliens L, Reijneveld JC, Taphoorn MJ. The end-of-life phase of high-grade glioma patients: A systematic review. Support Care Cancer 2014;22(3):847–57.
5. Jones-Rhoades MW, Bartel DP. Computational identification of plant microRNAs and their targets, including a stress-induced miRNA. Mol Cell 2004;14(6):787–99.
6. Hamed M, Spaniol C, Zapp A, Helms V. Integrative network-based approach identifies key genetic elements in breast invasive carcinoma. BMC Genomics 2015;16(5): S2.
7. Bao S, Wang X, Wang Z, Yang J, Liu F, Yin C. MicroRNA-30 mediates cell invasion and metastasis in breast cancer. Biochem Cell Biol. 2018;96(6):825–31.
8. Lin Z, Lu Y, Meng Q, Wang C, Li X, Yang Y, Xin X, Zheng Q, Xu J, Gui X, and others. miR372 promotes progression of liver cancer cells by upregulating erbB-2 through enhancement of YB-1. Mol Ther Nucleic Acids 2018;11: 494–507.
9. Oberg AL, French AJ, Sarver AL, Subramanian S, Morlan BW, Riska SM, Borralho PM, Cunningham JM, Boardman LA, Wang L, Smyrk TC, Asmann Y, Steer CJ, Thibodeau SN. miRNA expression in colon polyps provides evidence for a multihit model of colon cancer. PLoS One 2011;6(6):9.
10. Leidinger P, Backes C, Blatt M, Keller A, Huwer H, Lepper P, Bals R, Meese E. The blood-borne miRNA signature of lung cancer patients is independent of histology but influenced by metastases. Mol Cancer 2014;13:202.
11. Verghese ET, Drury R, Green CA, Holliday DL, Lu X, Nash C, Speirs V, Thorne JL, Thygesen HH, Zougman A, Hull MA, Hanby AM, Hughes TA. MiR-26b is down-regulated in carcinoma-associated fibroblasts from ER-positive breast cancers leading to enhanced cell migration and invasion. J Pathol. 2013;231(3):388–99.
12. Kato M, Goto Y, Matsushita R, Kurozumi A, Fukumoto I, Nishikawa R, Sakamoto S, Enokida H, Nakagawa M, Ichikawa T, Seki N. MicroRNA-26a/b directly regulate La-related protein 1 and inhibit cancer cell invasion in prostate cancer. Int J Oncol. 2015;47(2):710–8.
13. Miyamoto K, Seki N, Matsushita R, Yonemori M, Yoshino H, Nakagawa M, Enokida H. Tumour-suppressive miRNA-26a-5p and miR-26b-5p inhibit cell aggressiveness by regulating PLOD2 in bladder cancer. Br J Cancer 2016; 115(3):354–63.
14. Roelofs HM, Te Morsche RH, van Heumen BW, Nagengast FM, Peters WH. Over-expression of COX-2 mRNA in colorectal cancer. BMC Gastroenterol. 2014;14(1):14–1.
15. Misra S, Sharma K. COX-2 signaling and cancer: New players in old arena. Curr Drug Targets 2014;15(3):347–59.
16. Rodler D, Sinowatz F. Expression of prostaglandin-synthesizing enzymes (cyclooxygenase 1, cyclooxygenase 2) in the ovary of the quail (Coturnix japonica). Folia Biol. (Praha) 2015;61(4):125–33.
17. Walther U, Emmrich K, Ramer R, Mittag N, Hinz B. Lovastatin lactone elicits human lung cancer cell apoptosis via a COX-2/PPARgamma-dependent pathway. Oncotarget 2016;7(9):10345–62.
18. Che XH, Chen CL, Ye XL, Weng GB, Guo XZ, Yu WY, Tao J, Chen YC, Chen X. Dual inhibition of COX-2/5-LOX blocks colon cancer proliferation, migration and invasion in vitro. Oncol Rep. 2016;35(3):1680–8.
19. Bayomi EA, Barakat AB, El-Bassuoni MA, Talaat RM, El-Deftar MM, Abdel Wahab SA, Metwally AM. Cyclooxygenase-2 expression is associated with elevated aspartate aminotransferase level in hepatocellular carcinoma. J Cancer Res Ther. 2015;11(4):786–92.
20. Escuin-Ordinas H, Atefi M, Fu Y, Cass A, Ng C, Huang RR, Yashar S, Comin-Anduix B, Avramis E, Cochran AJ, Marais R, Lo RS, Graeber TG, Herschman HR, Ribas A. COX-2 inhibition prevents the appearance of cutaneous

squamous cell carcinomas accelerated by BRAF inhibitors. Mol Oncol. 2014;8(2):250–60.
21. Fujita M, Kohanbash G, Fellows-Mayle W, Hamilton RL, Komohara Y, Decker SA, Ohlfest JR, Okada H. COX-2 blockade suppresses gliomagenesis by inhibiting myeloid-derived suppressor cells. Cancer Res. 2011;71(7):2664–74.
22. Liu J, Ma L, Li C, Zhang Z, Yang G, Zhang W. Tumor-targeting TRAIL expression mediated by miRNA response elements suppressed growth of uveal melanoma cells. Mol Oncol. 2013;7(6):1043–55.
23. Xia M, Duan ML, Tong JH, Xu JG. MiR-26b suppresses tumor cell proliferation, migration and invasion by directly targeting COX-2 in lung cancer. Eur Rev Med Pharmacol Sci. 2015;19(24):4728–37.
24. Shen G, Lin Y, Yang X, Zhang J, Xu Z, Jia H. MicroRNA-26b inhibits epithelial-mesenchymal transition in hepatocellular carcinoma by targeting USP9X. BMC Cancer 2014;14:393.
25. Hugo HJ, Saunders C, Ramsay RG, Thompson EW. New Insights on COX-2 in chronic inflammation driving breast cancer growth and metastasis. J Mammary Gland Biol Neoplasia 2015;20(3–4):109–19.
26. Kang JH, Song KH, Jeong KC, Kim S, Choi C, Lee CH, Oh SH. Involvement of Cox-2 in the metastatic potential of chemotherapy-resistant breast cancer cells. BMC Cancer 2011;11:334.
27. Wu X, Cai M, Ji F, Lou LM. The impact of COX-2 on invasion of osteosarcoma cell and its mechanism of regulation. Cancer Cell Int. 2014;14:27.
28. Jana D, Sarkar DK, Ganguly S, Saha S, Sa G, Manna AK, Banerjee A, Mandal S. Role of cyclooxygenase 2 (COX-2) in prognosis of breast cancer. Indian J Surg Oncol. 2014; 5(1):59–65.
29. Sadaria MR, Yu JA, Meng X, Fullerton DA, Reece TB, Weyant MJ. Secretory phospholipase A2 mediates human esophageal adenocarcinoma cell growth and proliferation via ERK 1/2 pathway. Anticancer Res. 2013;33(4): 1337–42.
30. Wang XF, Zhou QM, Du J, Zhang H, Lu YY, Su SB. Baicalin suppresses migration, invasion and metastasis of breast cancer via p38MAPK signaling pathway. Anticancer Agents Med Chem. 2013;13(6):923–31.
31. Drigotas M, Affolter A, Mann WJ, Brieger J. Reactive oxygen species activation of MAPK pathway results in VEGF upregulation as an undesired irradiation response. J Oral Pathol Med. 2013;42(8):612–9.
32. Mirzoeva OK, Das D, Heiser LM, Bhattacharya S, Siwak D, Gendelman R, Bayani N, Wang NJ, Neve RM, Guan Y, Hu Z, Knight Z, Feiler HS, Gascard P, Parvin B, Spellman PT, Shokat KM, Wyrobek AJ, Bissell MJ, McCormick F, Kuo WL, Mills GB, Gray JW, Korn WM. Basal subtype and MAPK/ERK kinase (MEK)-phosphoinositide 3-kinase feedback signaling determine susceptibility of breast cancer cells to MEK inhibition. Cancer Res. 2009;69(2):565–72.